Film thickness investigation in heavily loaded hypoid gear pair elastohydrodynamic conjunctions

STLE
Dallas ★ May 17-21, 2015

Film Thickness Investigation in Heavily Loaded Hypoid Gear Pair Elastohydrodynamic Conjunctions

TRACK: Gears

AUTHORS: Leonidas Paouris, Loughborough University, UK

Stephanos Theodossiades, Loughborough University, UK

Miguel De la Cruz, Loughborough University, UK

Homer Rahnejat, Loughborough University, UK

Adam Kidson, Lubrizol Ltd., UK

Gregory Hunt, Lubrizol Ltd., UK

William Barton, Lubrizol Ltd., UK

INTRODUCTION

Hypoid gear pairs are some of the most highly loaded components of the differential unit in modern automobiles. Prediction of wear rate and generated friction require determination of lubricant film thickness. However, only very few investigations have addressed the issue of thin elastohydrodynamic films in hypoid gear pairs. The main reason for dearth of analysis in this regard has been the need for accurate determination of transient contact geometry and kinematics of interacting surfaces throughout a typical meshing cycle. Furthermore, combined gear dynamics and lubrication analysis of any pairs of simultaneous meshing teeth pairs is required. Simon [1] was among the first to deal with these issues. He used Tooth Contact Analysis (TCA) in order to calculate the instantaneous contact geometry and load for any teeth pair during their meshing cycle. However, in his study, the load carried by the hypoid pair was quite low, making the application of the results limited and not entirely suitable for real life operating conditions of typical hypoid gear pairs of vehicular differentials, which is of interest in the current paper.

Xu and Kahraman [2] performed numerical prediction of power losses and consequently the film thickness for highly loaded hypoid gear pairs. However, in their study only the one-dimensional Reynolds equation was employed. Consequently, the effect of lubricant side leakage in the passage through the contact was ignored. A more recent study by Mohammadpour *et al.* [3] employed realistic gear geometry data (through the use of TCA) for calculation of film thickness time history through mesh. The two-dimensional Reynolds equation, accounting for the side leakage of the lubricant, was solved numerically. It was shown that the side leakage component of the entraining velocity can significantly influence the film thickness.

With regard to hypoid gear dynamics, several studies should be mentioned. Wang and Lim [4] studied the dynamic response of hypoid gear pairs under the influence of time varying meshing stiffness. Yang and Lim [5] created a model able to predict the dynamic response of a hypoid gear pair by taking into account the lateral translations of their shafts due to the compliance of the supporting bearings. Karagiannis *et al.* [6-7] studied the dynamics of automotive differential hypoid gear pairs by taking into account the velocity dependent resistive torque at the gear caused by aerodynamic drag and tyre-road rolling resistance. The study integrated the gear dynamics with the generated viscous and boundary conjunctional friction.

THEORY AND GOVERNING EQUATIONS

Gear Dynamics

A 4 Degree-of-freedom torsional gear dynamics solver is employed in order to calculate the contact characteristics for each instant of a typical meshing cycle. The finite torsional stiffness of the pinion and the gear supporting shafts is also taken into account. Equations (1)-(4) are used to describe the torsional dynamics of the system.

$$\ddot{\varphi}_s = \frac{1}{I_s}\left[-k_t\left(\varphi_s - \varphi_p\right) - c_{t1}\left(\dot{\varphi}_s - \dot{\varphi}_p\right) + T_s\right] \qquad (1)$$

$$\ddot{\varphi}_p = \frac{1}{I_p}\left[-R_p(k_m f + c\dot{x}) + k_t(\varphi_s - \varphi_p) + c_{t1}(\dot{\varphi}_s - \dot{\varphi}_p)\right] \quad (2)$$

$$\ddot{\varphi}_g = \frac{1}{I_g}\left[R_g(k_m f + c\dot{x}) - k_t(\varphi_g - \varphi_w) - c_{t2}(\dot{\varphi}_g - \dot{\varphi}_w)\right] \quad (3)$$

$$\ddot{\varphi}_w = \frac{1}{I_w}\left[k_t(\varphi_g - \varphi_w) + c_{t2}(\dot{\varphi}_g - \dot{\varphi}_w) - T_w\right] \quad (4)$$

In equations (1)-(4), the backlash function f is calculated according to Kahraman and Singh [8] while the dynamic transmission error x and the resistive torque at the gear are calculated according to Karagiannis *et al.* [6]. The time varying contact characteristics are calculated for each time step, by employing the method used by Kahraman and Singh [8] as well as Karagiannis *et al.* [6]. In equations (1)-(4), φ_s, φ_p, φ_g and φ_w represent the angular displacements of the pinion shaft, the pinion, the gear and the gear shaft respectively. T_s and T_w are the constant input and the resistive torque respectively. R_p, R_g, k_t, k_m, c, c_{t1} and c_{t2} are the instantaneous contact radii of the pinion and the gear, the constant torsional stiffness of the pinion and the gear shafts, the time varying meshing stiffness, the damping coefficient of the mesh and the damping coefficients of the pinion and the gear shafts respectively.

Elastohydrodynamic Teeth Pair Conjunctions

In order to estimate the film thickness throughout the meshing cycle, an (elliptical) point contact EHL solver is developed. It is assumed that the lubricant exhibits Newtonian shear behavior. This assumption will lead to sufficiently accurate estimations of the film thickness, since the film thickness is mostly influenced by the inlet boundary conditions under elastohydrodynamic conditions and is rather insensitive to load. Also, the current analysis is isothermal and inlet shear heating is not considered at this stage. The 2D Reynolds equation is solved numerically in order to determine the lubricant pressure distribution [9]:

$$\frac{\partial}{\partial x}\left[\frac{\rho h^3}{\eta}\frac{\partial p}{\partial x}\right] + \frac{\partial}{\partial y}\left[\frac{\rho h^3}{\eta}\frac{\partial p}{\partial y}\right] = 6\left\{\frac{\partial}{\partial x}[\rho h(U_1 + U_2)] + \frac{\partial}{\partial y}[\rho h(V_1 + V_2)] + 2\frac{d(\rho h)}{dt}\right\} \quad (5)$$

The value of the film thickness at each point of the contact can be calculated using equation (6). The calculation of the local elastic deflection due to the pressure of the lubricant can be performed by numerical integration of the elasticity potential equation [10].

$$h(x, y) = h_0 + g(x, y, R_x, R_y) + \delta(x, y, p) \quad (6)$$

Finally, the pressure dependence of the low shear dynamic viscosity of the lubricant is calculated using Roelands equation [11]. In equation (5), p, h, ρ, and η are the pressure, film thickness, lubricant density and its low shear dynamic viscosity respectively. U_1, U_2, V_1 and V_2 represent the surface velocities at the point of contact of the pinion and the gear teeth. These are obtained through TCA.

RESULTS-CONCLUSIONS

The numerical results from the torsional gear dynamics model were used in order to calculate the contact load, the surface velocity of the teeth in meshing action as well as the local radii of curvature at the contact point. Table 1 summarizes the conditions within the meshing cycle locations studied along with the corresponding contact conditions.

Point	W (N)	U (m/s)	V (m/s)	Rzx (m/s)	Rzy (m/s)
1	652.14	2.240	3.655	0.0170	1.198
2	1778.11	2.289	3.447	0.0179	1.222
3	3016.08	2.265	3.069	0.0183	1.280
4	4679.21	2.286	2.922	0.0191	1.299
5	5142.83	2.326	2.790	0.0196	1.302
6	5323.86	2.346	2.690	0.0199	1.310
7	5005.89	2.344	2.656	0.0200	1.320
8	4198.77	2.340	2.628	0.0201	1.330
9	449.01	2.448	2.202	0.0224	1.329

Table 1: Points of the Meshing Cycle under study

The numerical results regarding the film thickness contour for points 1, 5 and 9 of the meshing cycle are illustrated in figure 1. The values presented in table 1 correspond to the input variables of the EHL code.

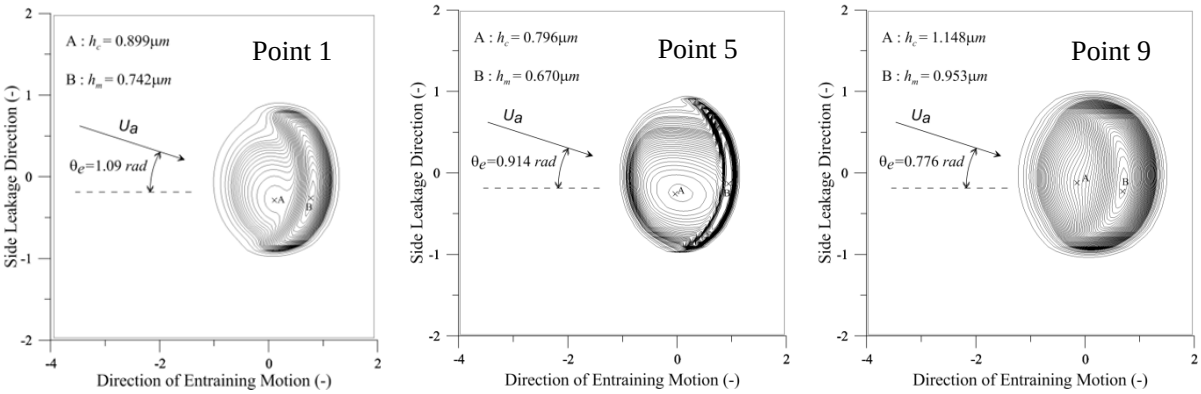

Figure 1: Film thickness contours for Points 1, 5 and 9 in the meshing cycle

An important point to note is that the lubricant is entrained into the contact at an angle. Thus, a significant proportion of the flow results in side leakage, which is often not taken into account in many analyses of hypoid gear pair lubrication studies. As it can be seen in figure 1, the horse-shoe shaped minimum film exit constriction shifts to the rear of the Hertzian contact domain with an increasing contact load as it would be expected. At the same time, the magnitudes of the entraining and the side leakage velocity remain almost the same for all the points examined (see table 1). The side leakage component of the entraining velocity causes an asymmetry on the total entraining velocity distribution in the conjunction, which in turn leads to an asymmetry in the lubricant film contours. It is observed that the point of minimum film thickness is displaced downstream with respect to the component of the side leakage velocity. It is also apparent that, at least for the highly loaded point 5, the region of the film thickness which corresponds to the exit constriction, and hence the minimum film thickness, is only a small proportion of the total area of contact which lies inside the equivalent Hertzian contact ellipse. The film thickness for the rest of the contact zone can be characterized by the value of the central film thickness. Finally, the film thickness distribution for point 9, which is the point with lowest load, whilst with similar entraining velocity shows a gradual shift away from piezo-viscous elastic (EHL) towards hydrodynamics. A comparison between the values of the central and minimum film thickness and the corresponding values determined using the Chittenden-Dowson equation [12] is presented in figure 2. It should be noted that the inlet fully-flooded/starved boundary position was checked against starvation boundary determined by Hamrock and Dowson [13] for all the meshing points considered. The fully-flooded/starved boundary position is located at a distance of $2b - 3b$ from the centre of the contact ellipse and along the direction of entraining motion. It should be noted that the theory behind the calculation of this boundary position does not take into account the presence of angled flow. The side leakage component of the flow may be able to move the inlet meniscus position, which may have consequences on the fully-flooded/starved boundary position predicted by the existing theory [13]. In order to securely prevent the presence of starvation in the numerical results, an inlet distance of $4b$ was set throughout the analysis.

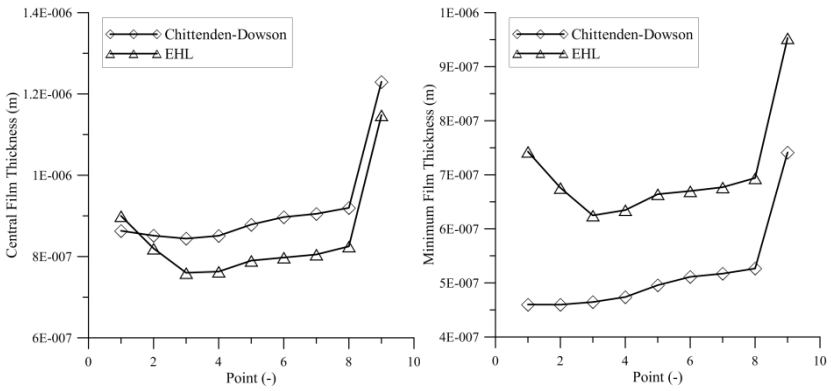

Figure 2: Central (left) and minimum (right) film thickness for the points examined

As seen in figure 2, the central film thickness values calculated using the present EHL numerical solver show good agreement with the central film thickness predicted using the Chittenden-Dowson equation for the

conditions examined. For the majority of the highly loaded points (points 3-8) the difference between the numerically predicted central film thickness values and those of the extrapolated film thickness equation is around 10%. The extrapolated equation seems to overestimate the central film thickness. For the lightly loaded points 1, 2 and 9 the numerical results for the central film thickness show better agreement with those of Chittenden-Dowson equation. Almost the same trend is noted for the case of minimum film thickness. However, the difference between the analytical and the numerical results is around 30%.

ACKNOWLEDGMENTS

The authors would like to express their gratitude to Lubrizol Ltd. for the financial support of this project.

REFERENCES

[1] Simon, V., 1981, "Elastohydrodynamic Lubrication of Hypoid Gears," *J. Mech. Des.*, **103**, pp. 195–203.

[2] Xu, H., and Kahraman, A., 2007, "Prediction of friction-related power losses of hypoid gear pairs," *Proc. Inst. Mech. Eng. Part K J. Multi-body Dyn.*, **221**(3), pp. 387–400.

[3] Mohammadpour, M., Theodossiades, S., and Rahnejat, H., 2012, "Elastohydrodynamic lubrication of hypoid gear pairs at high loads," *Proc. Inst. Mech. Eng. Part J J. Eng. Tribol.*, **226**(3), pp. 183–198.

[4] Wang, J., Lim, T., C., and Li, M., 2007, "Dynamics of a hypoid gear pair considering the effects of time-varying mesh parameters and backlash nonlinearity," *J. Sound Vib.*, **308**(2), pp. 302–329.

[5] Yang J., and Lim, T., 2011, "Dynamics of Coupled Nonlinear Hypoid Gear Mesh and Time-varying Bearing Stiffness Systems," *J. Passeng. Cars*, **4**(2), pp. 1039–1049.

[6] Karagiannis, I., Theodossiades, S., and Rahnejat, H., 2012, "On the dynamics of lubricated hypoid gears," *Mech. Mach. Theory*, **48**, pp. 94–120.

[7] Karagiannis I., and Theodossiades, S., 2013, "An Alternative Formulation of the Dynamic Transmission Error to Study the Oscillations of Automotive Hypoid Gears," *J. Vib. Acoust.*, **136**(1), pp. 1–12.

[8] Kahraman A., and Singh, R., 1990, "Non-Linear Dynamics of a Spur Gear Pair," *J. Sound Vib.*, **142**, pp. 49–75.

[9] Reynolds, O., 1886, "On the Theory of Lubrication and Its Application to Mr. Beauchamp Tower's Experiments, Including an Experimental Determination of the Viscosity of Olive Oil," *Proc. R. Soc. London*.

[10] Timoshenko S., and Goodier, J., N., 1951, "Theory of Elasticity," *McGraw-Hill B. Co*.

[11] Roelands, C., 1966, "Correlational Aspects of the Viscosity-Temperature Pressure Relationship of Lubricating Oils,".

[12] Chittenden, R., J., Dowson, D., Dunn, J., F., and Taylor, C., M., 1985, "A Theoretical Analysis of the Isothermal Elastohydrodynamic Lubrication of Concentrated Contacts. I. Direction of Lubricant Entrainment Coincident with the Major Axis of the Hertzian Contact Ellipse," *Proc. R. Soc. A Math. Phys. Eng. Sci.*, **397**, pp. 245–269.

[13] Hamrock B., J., and Dowson, D., 1977, "Isothermal Elastohydrodynamic Lubrication of Point Contacts Part IV — Starvation Results," *J. Lubr. Technol.*, pp. 15–23.

KEYWORDS: EHL, Gear Geometry, Gear Dynamics, Lubricant Film Thickness